Nuclear Instruments and Methods in Physics Research A 724 (2013) 27–33

Contents lists available at SciVerse ScienceDirect

Nuclear Instruments and Methods in Physics Research A

journal homepage: www.elsevier.com/locate/nima

Spectrometric performances of high quantum efficiency multi and single anode PMTs coupled to LaBr3(Ce) crystal

Maria Nerina Cinti [a,b,*], Roberto Pani [a,b], Rosanna Pellegrini [a,b], Paolo Bennati [a], Chiara Orlandi [c], Andrea Fabbri [d,e], Stefano Ridolfi [a], Raffaele Scafè [a]

[a] Department of Molecular Medicine, Sapienza University of Rome, Rome 00161, Italy
[b] INFN Rome 1 Section, Rome, Italy
[c] Medical Physics Post Graduate School, Sapienza University of Rome, Rome 00161, Italy
[d] Department of Physics, Roma Tre University, Rome, Italy
[e] INFN Rome 3 Section, Rome, Italy

ARTICLE INFO

Article history:
Received 27 October 2012
Received in revised form
25 March 2013
Accepted 12 April 2013
Available online 4 May 2013

Keywords:
Gamma detector
Spectroscopy
Multi anode PMT
Scintillation crystall

ABSTRACT

High quantum efficiency semiconductor photodetectors have recently drawn the attention of the scientific community for their potential in the realization of a new class of scintillation imagers with very high energy and spatial resolution performance. However, this goal does not seem within easy reach, due to various technological issues such as, for example, the difficulty to scale the characteristics of a single detector to an imager with suitable dimensions. Lately a definite technical improvement in increasing quantum efficiency up to 42% for position sensitive photomultipliers was achieved. The aim of this work is thus to test this new technological progress and to study the possible implications in imaging applications. Four Hamamatsu PMTs were tested: two multi anode photomultipliers, one with a bialkali (27% quantum efficiency) and the other one with a super-bialkali photocathode (38% quantum efficiency), and two 1×1 in. PMTs, both equipped with an ultra bialkali photocathode (42% quantum efficiency). In particular one of the ultra bialkali PMT has also an increased efficiency of first dynode charge collection. The results were compared with the ones obtained with a reference PMT (Hamamatsu R6231), mainly used in spectroscopy. The PMTs were coupled to LaBr3(Ce), NaI(Tl) and LSO(Ce) continuous scintillation crystals. The tests were done using two independent electronic chains: one dedicated for spectroscopic application and a second one, using a multi wire 64 channel readout, for imaging applications. The super-bialkali MA-PMTs have shown high energy resolution, both with spectroscopic and imaging setup, highlighting the appropriateness of these devices for the development of imaging devices with high spectroscopic performance.

1. Introduction

Recently the attention of the scientific community focused on the important results in terms of energy and spatial resolution obtained by semiconductor photodetectors (SP) characterized by high quantum efficiency (HQE). A QE enhancement was also achieved in photomultipliers (PMTs) and multi anode PMTs (MA-PMTs), in order to improve the performances of these photodetectors and, as a consequence, to obtain competitive results with respect to semiconductor photodetectors. In this work we show the response in term of Full Width Half Maximum Energy Resolution (ER) of new Super BiAlkali (SBA) MA-PMT and Ultra BiAlkali (UBA) PMT, developed by Hamamatsu, to establish the topicality of these photodetectors compared to the emerging semiconductor ones. To justify this statement, we start summarizing and discussing the main characteristics and ER results of devices based on SP photodetectors coupled to scintillation crystals, both for spectroscopy and for imaging applications (see Table 1).

Table 1 shows that the scintillation crystals mainly used with SP are LSO (Ce) and CsI(Tl), due to the correspondence between the maximum light yield of crystals and the maximum of the QE distribution of semiconductor devices, as shown in Fig. 1 where the QE of principal photodetectors and the light yield of the principal scintillation crystals are represented as a function of the wavelength.

For applications requiring scintillation crystals with high light production and short decay time, like LaBr3(Ce), or cheaper and more conventional crystal like NaI(Tl), the effective QE of semiconductor devices is comparable with one of Ultra BiAlkali PMT (about 40%, as shown in Fig. 1).

* Corresponding author at: Sapienza University of Rome, Department of Molecular Medicine, Viale Regina Elenea 291, 00161 Rome, Italy. Tel.: +390649918277; fax: +390649918277.
E-mail address: marianerina.cinti@uniroma1.it (M.N. Cinti).

0168-9002/$ - see front matter © 2013 Elsevier B.V. All rights reserved.
http://dx.doi.org/10.1016/j.nima.2013.04.045

Table 1
Energy resolution results of the main semiconductor devices.

Photodetector	Scintillation crystal	Energy resolution	Temperature	QE	Size	Ref.
Silicon Drift	CsI(Tl)	6.10% @122 keV	−15 °C	95% @550 nm	1 cm^2 active area	[1]
Silicon Drift	LaBr3(Ce)	5.70% @ 120 keV 2.70% @662 keV	−0 °C Room	95% @550 nm	– –	[2]
Silicon Drift	CsI(Tl)	14% @122 keV	−10 °C	85% @550 nm	1 cm^2 active area	[3]
Avalanche PhotoDiode (Hamamatsu)	CsI(Tl)	4.90% @662 keV	−20 °C	≥80% @500–830 nm 60% @390 nm	10 × 10 mm^2	[4]
Si–APD	CsI(Tl)	15.60% @122 keV 7.70% @662 keV	Room		5 × 5 mm^2 active area	[5]
Si–APD	LaBr3(Ce)	23.10% @ 122 keV 7.30% @662 keV	Room	≥80% @500–830 nm 60% @380 nm	5 × 5 mm^2 active area	[5]
SiPM (Hamamatsu)	LSO	12.10% @662 keV	Room	20–30% (PDE)	3 × 3 mm^2 active area	[6]
SiPM	LSO	35% @511 keV			1 × 1 mm^2 active area	[7]
APD (Hamamatsu)	LSO	19.75 (CFoV) @511 keV	Room	55% @420 nm	3 × 3 mm^2 active area	[8]

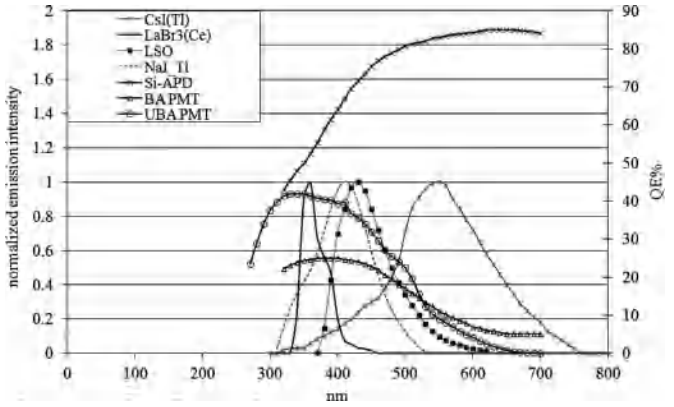

Fig. 1. Normalized emission intensity of principal scintillation crystal and quantum efficiency of photodetector devices as a function of the wavelength. The quantum efficiency percentage curves for photodetectors are obtained by Hamamatsu technical sheets.

For medical gamma imaging applications, like biodynamic studies, or applications where a short scintillation time is important (for an example in PET), Cs(Tl) scintillation crystal is unsuitable, due to the long decay time and the presence of afterglow, that causes pulse pileup in high count-rate applications, reduced energy resolution and artifacts in tomography applications. [9].

In addition, some results in Table 1 are obtained at low temperature, highlighting the dependence of the SP from cooling systems.

Finally, we consider the available active area, which is an important parameter in the development of gamma imagers. Currently the active area obtainable for a gamma imager based on SP is less than 10 cm^2, with a large number of elements for area unit (for example, 77 in DRAGO [10]), and the related high number of electronic chains, affecting the performance and cost of the overall detector. On the contrary, the new generation of MA-PMTs based on metal channel technology is designed to facilitate the assembly in arrays, thanks to the reduced dead zone among the tubes; as a consequence there are no limits in the overall achievable size of the gamma detector. Furthermore, the number of the electronic outputs of these photomultipliers is comparatively smaller: the H8500 MA-PMT has 64 outputs for two inch square active area. As an example of the application of this new generation of PMT/MA-PMT, our team has recently developed a multiple gamma camera [12–15] with an array of 6 × 7 PMTs, based on metal channel technology and with BA photocathode, coupled to a pixellated NaI(Tl) scintillator crystal (42 inch square overall active area and 42 channels electronic readout). Moreover, we are testing a new compact high resolution gamma camera based on a 2 × 2 array of two inch square active area MA-PMTs[16] with SBA photocathode, coupled to a continuous LaBr3(Ce) crystal, with 100 cm^2 active area and 256 channels electronic readout.

From the considerations made so far, we can deduce that the use of PMT is still competitive in the areas of interest discussed above.

The focus of this work is highlighting the good linearity response and the suitable energy resolution results of new HQE PMTs/MA-PMTs, developed by Hamamatsu [11], when coupled to scintillation crystals like LaBr3(Ce), NaI(Tl) and LSO(Ce), in comparison with the ones obtained with PMT/MA-PMT with standard photocathode (BA). Furthermore the results from the new UBA PMT prototype (one inch square active area) by Hamamatsu with enhanced efficiency of first dynode charge are reported, in order to evaluate the effect on the energy resolution of this implementation.

2. Equipment and method

In this work two groups of scintillation crystals were used. The first group consists of two continuous crystals, a LaBr3(Ce) and a NaI(Tl), with the same size (51 × 15 × 4 mm^3+3 mm glass window) and treatment of surfaces planned for imaging application (white painted on the back side and black painted on the edge). The second group includes a 1/2 inch diameter LaBr3(Ce) cylinder and

a LSO cube, 1 in. side, white painted on all surfaces except at the output window, planned for spectroscopy applications. The size of these last two crystals was selected in order to optimize the coupling to one inch square area PMTs (R7600U-200 and R11625). To distinguish between the two LaBr3(Ce) crystals, the one for imaging application will be indicated with LaBr_img while the cylindric one with LaBr_cyl. The details of the scintillation crystals are summarized in Table 2.

The list and characteristics of the PMTs are given in Table 3, all produced by Hamamatsu [11].

In order to contrast the effect of dynode current saturation due to the high light production and short decay time of LaBr3(Ce) crystal [17], two different techniques have been deployed: the use of a tapered voltage divider, like for R11265, R6231 and UBA R7600U-200 photomultipliers, and the reduction of the number of dynode stages, applied on H8500C-100 MOD8 MA-PMT, where this number was reduced to 8 respect to 12 of the standard H8500 one.

Two distinct electronic readouts were used: a spectrometry equipment based on an ORTEC mod.113 preamplifier and a customized amplifier-shaper with a fast time constant suitable for LaBr3(Ce) decay time. Energy spectra were recorded by an ORTEC mod. 916A Multi Channel Buffer PC card. To evaluate the energy resolution performance of MA-PMT with this spectroscopic chain, the 64 outputs of the photomultiplier were reduced to only one signal (short circuit configuration).

The second equipment, for imaging applications, is based on a 64 channel anode read out (multi-anode configuration) developed by University of Roma 3 [18]. All the anodes are independently read and digitized (through a 14 bit ADCs) with a maximum sampling frequency of 250 ksample/s. The front-end is based on an operational amplifier in Charge Sensitive (CSA) configuration. The event selection is made by the digital control implemented in a FPGA, that analyzes the data read in each time slot and discards those below a given threshold. The analog frontends are organized in PCBs with 16 channels each, and the system modularity makes possible working with 4 analog PCB (64 channel for H8500 PMTs). The FPGA and the voltage regulators are housed on docking PCB. The FPGA board has a 100 MHz clock for data acquisition and the data transmission is operated via USB 2.0.

The characteristics of both electronic readouts are summarized in Table 4.

The response linearity and energy resolution were evaluated for all detectors in the energy range 32–1330 keV, using 3 mm diameter collimated sources.

In a previous work [19] the pulse height linearity of all PMTs involved in this work was tested also as a function of photon energy and high voltage (HV) supply. Furthermore the effect of the tapered voltage divider or the reduction of number of dynode stages was evaluated, demonstrating the effectiveness of these technological modifications to correct the predicted non-linearity effects on LaBr3(Ce) response at high photon energy, due to its

Table 2
Scintillation crystals.

Scintillation crystal	Active area (mm^2)	Thickness (mm)	Density (gr/cm^3)	Light yield (photon/MeV)	Decay time (ns)	Emission peak (nm)	Note
LaBr3(Ce) Continuous (Saint Gobain)	51.0 × 51.0	4	5.07	63000	16	380	White paint on back Black paint on edges (for imaging) (LaBr_img)
LaBr3(Ce) Continuous (Saint Gobain)	12.5 Ø	12.5	5.07	63000	16	380	White paint on back and edges (LaBr_cyl)
NaI(Tl) Continuous (Hilger)	51.0 × 51.0	4	3.67	38000	230	410	White paint on back Black paint on edges (for imaging)
LSO(Ce) Continuous(Hilger)	11.4 × 11.4	12.4	7.35	25000	40	420	White carbon polymeric film on back and edges

Table 3
Characteristics of the utilized Hamamatsu PMTs.

Photodetector	Dynode stages	Quantum Efficiency (@ 380 nm)	Efficiency of first dynode charge collection	Size (mm^2)	Dynode structure	Gain Typ ($\times 10^6$)	Voltage divider
R6231-01 Standard PMT	8	30.00%	80%[19]	51Æ	Linear Focused	0.27	Tapered (ID.AS20 by S.Gobain)
R7600U-200 Standard PMT	10	43.80% "UBA"	70%	25 × 25	Metal Channel	1	Tapered (ID. E5996 by Hamamatsu)
R11265 Standard PMT	10	42.70% "UBA"	90%	25 × 25	Metal Channel	1	Not tapered
H8500C MA-PMT (old Part Number)	12	27.00% "BA"	70%	51 × 51	Metal Channel	2	Not tapered
H8500C-100 MOD8 MA-PMT (old Part Number)	8	38.70% "SBA"	70%	51 × 51	Metal Channel	0.27	Not tapered

Table 4
Characteristics of both electronic readouts.

Electronic readouts	Channels	Note
Multianode	64	4 analogic PCBs A backbone PCB for the analog PCB interconnection and the delivery of the power supply A FPGA board with a 100 MHz clock for data acquisition A CPU for PC data transmission via USB 2.0 14 bit resolution
Spectrometry	1	ORTEC mod.113 preamplifier and a custom amplifier ORTEC mod.916A multi channel buffer PC card

high light yield and short decay time. Finally a procedure of local calibration of linearity curve in pulse height was optimized in order to correct possible non linear residual effects [19]. This procedure was applied also in this work. According to the optimized results in term of energy resolution and pulse height linearity response reported in [19], the HV supply of both H8500 MA-PMTs and R6231 PMTs was set to 1000 V while for R7600U-200 and R11265 PMTs to 900 V.

The *ER* consists of three contributes: intrinsic, electronic and statistical.

$$ER = \sqrt{(ER_{\text{intrisic}})^2 + (ER_{\text{electronics}})^2 + (ER_{\text{statistical}})^2} \quad (1)$$

We have shown in [19] that the spectroscopic readout contribution to the $ER_{electronic}$ term is negligible. Furthermore the multi wire readout was designed with uncoupled channels, to get electronic noise close to poissonian statistic, estimated less than 1% [18].

Regarding the *ER* intrinsic term, the LaBr3(Ce) scintillator gives a limited and well defined contribution to the energy resolution, as shown in [20]. In particular at 140 keV the intrinsic energy resolution is about 4%.

The *ER* statistical term in (1) can be represented by [20]:

$$ER_{\text{stat}} \propto \frac{2.35}{\sqrt{N_p he}} = \frac{2.35}{\sqrt{QE \times \delta}} \times N \quad (2)$$

where N is the number of photons produced and arrived at the photocathode, QE is the quantum efficiency of the photocathode and δ is the efficiency of photoelectron collection at the first dynode. So the effect of an enhanced QE or efficiency of first dynode is directly related to this statistical term.

Then, based on the above considerations, the use of the proposed electronic readouts and the LaBr3(Ce) crystal could be the best way to highlight the effect of the PMT characteristics on the energy resolution results. These results were also compared to the ones obtained with a NaI(Tl) crystal, which is commonly used in molecular imaging applications.

The energy resolution results from BA, SBA and UBA PMTs were compared to investigate the role of the enhanced quantum efficiency in energy resolution evaluation. As shown in Table 3, the δ factor is similar in all PMTs, except for the R11265 one; so, using the same scintillation crystal and electronic readout, it is possible to evaluate directly the effect of enhanced QE in ER values. According with (2) and with the data reported in Table 3, the ratio between the ER values obtained for example with SBA and BA PMT is summarized by:

$$\frac{ER_{SBA}}{ER_{BA}} \propto \sqrt{\frac{QE_{BA}}{QE_{SBA}}} = 83.5\% \quad (3)$$

Consequently a 16.5% maximum improvement of the energy resolution statistical term is expected for SBA PMT with respect to BA, while using an UBA PMT the expected improvement is about 21%. Regarding R11265 tube, also due to the increased efficiency of first dynode, the expected improvement should be about 30%. In Table 5 the expected improvements in ER_{stat} of the overall PMTs respect to the BA one are summarized.

Table 5
Expected maximum improvement in energy resolution statistical term with respect to BA PMT.

Photodetector	
H8500C-100 MOD8 (SBA)	−16.50%
R7600U-200 (UBA)	−21%
R11265 (UBA)	−30%

The energy resolution results from SBA and UBA PMTs were compared to the ones obtained with the standard PMT R6231, considered as a gold standard for spectroscopy applications.

A consideration has to be done regarding the poor match between the light yield distribution of $LaBr_3$:Ce crystals and the spectral quantum efficiency of R6231 PMT (380 and 404 nm, respectively [21]). Due to the high collection efficiency and QE, ER values from R6231 PMT coupled to LaBr3(Ce) crystal are expected to be close to the ones from SBA MA-PMT.

Finally the SBA PMT has been coupled with a LSO(Ce) crystal, typically used with semiconductor devices, to compare the performance of this photodetector with the semiconductor one.

3. Results and discussion

3.1. Results with spectroscopic electronic readout

In this measurements the MA-PMTs were set in short circuit configuration. In Fig. 2 the energy resolution results from all PMTs are shown, optically coupled with a LaBr_img, except for UBA and R11265 that were coupled to LaBr_cyl. A theoretical curve representing a poissonian behavior proportional to 1/sqrt(E) is overlapped. Fig. 2 shows that the good linearity of PMT response made possible to emphasize the expected effect of the higher QE of SBA (with respect to BA) on the ER value.

The predicted improvement in ER (see Table 5) for R7600U-200 UBA PMT is not achieved: the results obtained by this tube are very close to the ones by SBA, and therefore lower than the 20% calculated by the QE nominal values. This is probably due to the different scintillation crystal properties (LaBr_img respect to LaBr_cyl), not only associated to the different treatment of crystal surface but also in relation to the year of fabrication (the LaBr_Cyl is older than LaBr_img crystal) and the related accuracy in crystal growing process.

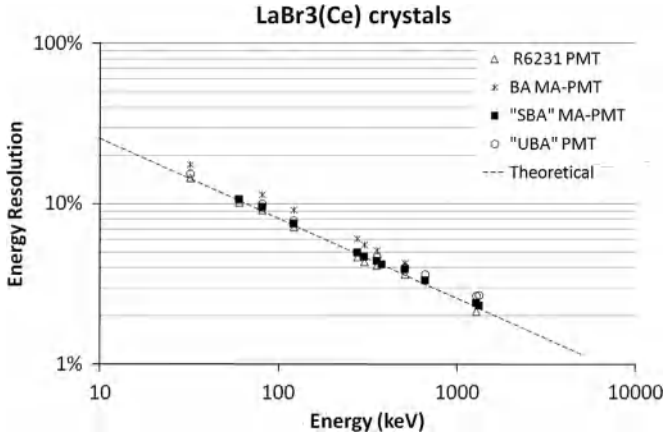

Fig. 2. Energy resolution results from LaBr3(Ce) scintillation crystals coupled to different photomultipliers.

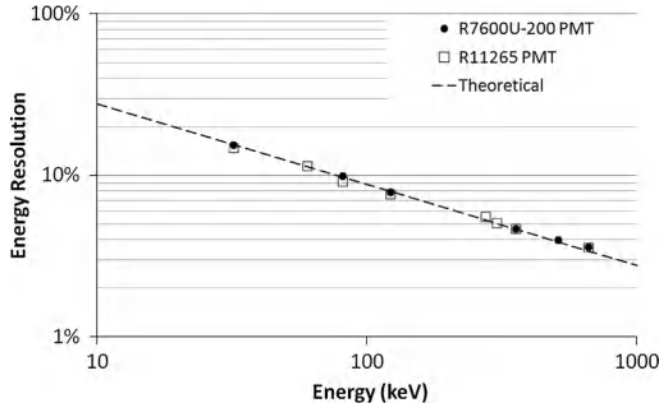

Fig. 3. Energy resolution obtained from ultra bialkali PMT (R7600U-200 and R11265), both coupled to LaBr3(Ce) cylinder for spectroscopic applications.

To better investigate the response of UBA PMTs, a direct comparison between R7600U-200 and R11265 PMT results is shown in Fig. 3, both coupled to LaBr_cyl. This way the comparison is strictly related to the evaluation of the characteristics of both photomultipliers. Furthermore an improvement in ER result is expected for R11265 due to the enhanced efficiency of first dynode (see Table 5).

The figure shows unexpectedly close ER values. This effect could be due to a inhomogeneity of response of photocathode for UBA PMTs, that could have contributed also to the non optimized response respect to SBA PMTs. A private communication with Hamamatsu regarding R11265 prototype confirmed an inhomogeneity of the relative output current of photocathode of about 35% as a function of the position of the detected event. The same parameter could not be verified for R7600U-200 PMT. A future experiment could be foreseen to check this assumption with the help of a small crystal scintillator coupled to different places of the PMT photocathode.

In any case these results have been also caused by the intrinsic behavior of LaBr3(Ce) crystal. To verify this statement, in Fig. 4 the ER results given by BA MA-PMT coupled to both LaBr3(Ce) and NaI(Tl) scintillation crystals are compared.

The NaI(Tl) scintillation crystal intrinsic ER component shows three different trends [22]: the first one, up to 100 keV photon energy, is close to a poissonian law; in the second, due to the light yield non proportionality component, the intrinsic ER component is constant up to 300 keV photon energy and finally it decreases slowly. This behavior is exactly shown in Fig. 4, demonstrating that

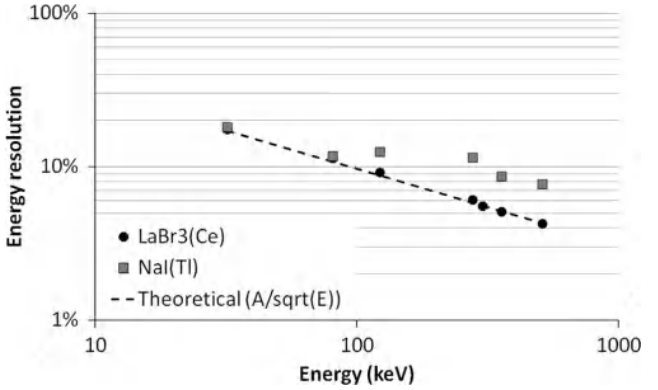

Fig. 4. Energy resolution results with bialkali multi anode photomultiplier coupled to LaBr3(Ce) and NaI(Tl) scintillation crystals.

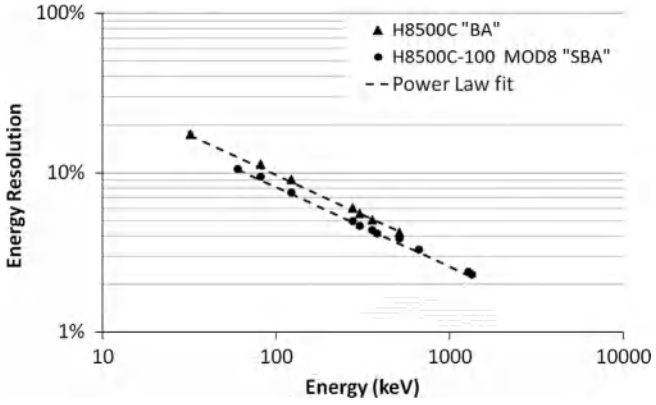

Fig. 5. Energy resolution from bialkali and super biakali multi anode photomultiplier coupled to continuous LaBr3(Ce) crystal for imaging application.

Table 6
Energy resolution results from MA-PMT and standard PMT's (% FWHM).

Photodetector	ER% @122keV	ER% @511 keV
H8500C-100 MOD8	7.5	4
H8500C	9	4.3
R7600U-200	7.8	3.9
R6231	7.2	3.6
R11265	7.7	4

only the LaBr3(Ce) crystal permits to enhance the difference in the characteristics of the PMTs reported in Fig. 2.

Fig. 5 shows the direct effect of photocathode QE on ER values, comparing BA and SBA MA-PMT, both coupled to LaBr_img. The two behaviors are fitted with a power law according to Eq. (2). Two proportional coefficients were selected, 1.00 ± 0.06 and 0.88 ± 0.15 for BA and SBA MA-PMT, respectively, and used to evaluate the improvement in the overall ER obtaining about −12%. These results are in agreement with the one reported in Table 5, considering that the improvement expected for only ER_{stat} term was −16.5% and depends exclusively by QE enhancement. So the linearity in response of these PMTs and the response of this scintillation crystal permit to optimize the effect of the improved quantum efficiency.

In order to visualize numerically the energy resolution results obtained with spectroscopic electronic readout and for comparison with the results obtained with semiconductor devices reported in Table 1, in Table 6 are summarized the values obtained with LaBr3(Ce) crystal at photon energy particularly interesting for

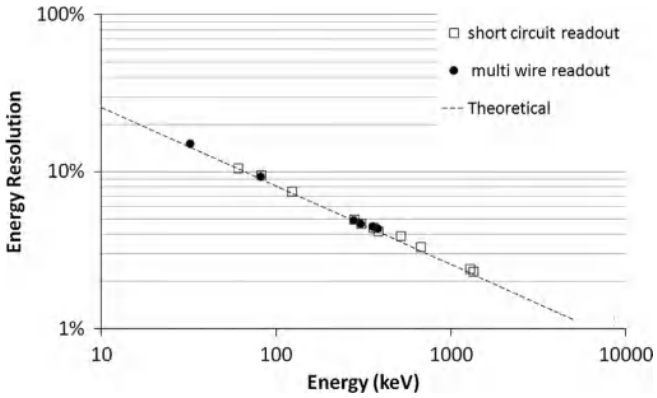

Fig. 6. Energy resolution obtained from super biakali multi anode photomultiplier coupled to continuous LaBr3(Ce) crystal for imaging application. The outputs of photomultiplier were read by short circuit and multi wire readout. The results are compared to the theoretical Poisson curve.

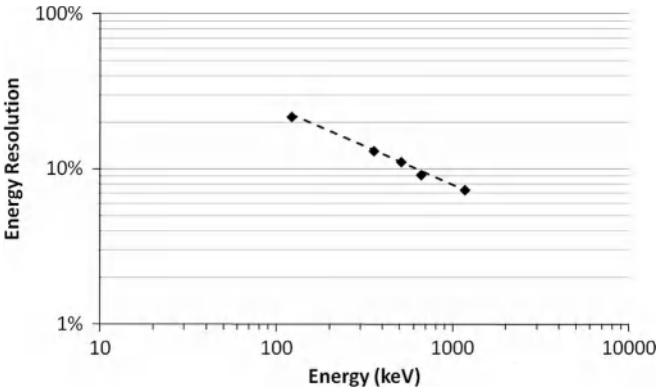

Fig. 7. Energy resolutions of super biakali multi anode photomultiplier, coupled with LSO(Ce) and read by multi wire readout.

medical applications, for instance in SPECT (122 keV) and PET (511 keV).

3.2. Results with multi wire electronic readout

As described in Section 2, the multi wire electronic readout used for these measurements presents a low electronic noise. Fig. 6 shows the energy resolution values to compare directly the different response of the SBA MA-PMT coupled to LaBr_img with both readouts.

Also in this case the results are very similar, demonstrating that the electronic readout does not affect the performance of MA-PMT. This conclusion is very important for imaging applications because a gamma detector based on a MA-PMT, coupled to LaBr3(Ce) crystal and multi wire readout having very high performance in terms of low noise, enables a good discrimination in energy, useful to remove scattering events to the advantage of image contrast. In particular in Single Photon Emission applications, as for example scintimammography, a good energy resolution allows to discriminate the scattering events originated by the body and, as a consequence, to achieve a high contrast of the image even in the area very close to the chest. Another application could be dual isotope SPECT technique, for myocardial or brain imaging, where two isotopes, typically Tc99m and I123, with similar photon energy, 140 and 160 keV, respectively, are used.

Finally, H8500 SBA MA-PMT was coupled to a LSO(Ce) to test the performance with a scintillation crystal typically used with semiconductor devices. The resulted energy resolution values are shown in Fig. 7.

Table 7
Energy resolutions of SBA, coupled with LSO(Ce).

Photon energy (keV)	Energy resolution	
	LSO+SBA MA-PMT (%)	Literature data (%)
122	21.70	
356	13.03	15.0[23] 13.5[8]
511	11.10	
662	9.19	8.4[24]
1174	7.32	

These values were compared with some results obtained with LSO(Ce) coupled to semiconductor device or photomultiplier, as reported in literature (see Table 7).

The only ER value better than the one obtained with SBA MA-PMT was with R6231 PMT, optimized for spectroscopic applications: $8.4 \pm 0.5\%$ [24] respect to $(9.2 \pm .2\%)$ at 662 keV. These results are very satisfactory considering that the light yield maximum for LSO does not fit with the QE maximum of SBA PMT (see Fig. 1). The results from SBA MA-PMT with LSO(Ce) are comparable with the ones from semiconductor and dedicated spectroscopic devices, further demonstrating that the new generation of MA-PMT is competitive in the overall scenario of gamma ray detectors.

4. Conclusions

In this work the spectroscopic results obtained with high quantum efficiency mono/multi anode photomultiplier coupled to LaBr3(Ce), NaI(Tl) and LSO(Ce) scintillation crystals are presented. The results show the suitable behavior of these photodetectors also with respect to semiconductor photodetectors. Multi anode photomultipliers have shown a very good linearity as a function of the photon energy also when used in imaging configuration.

The importance of imagers with high energy resolution relies in the possibility to discriminate the scattering events to improve the signal to noise ratio and the contrast of the image, to make visible lesions that would be otherwise obscured by the diffuse component. Furthermore high resolution performance enables the improvement of innovative single photon emission techniques like dual isotope imaging, where two isotopes with close photon energy are utilized. Detectors for this application require necessarily a high energy discrimination. The results have highlighted the importance of photomultiplier parameters like efficiency in first dynode charge collection and homogeneity in photocathode response in energy resolution performance. In a future scenario, a photomultiplier with ultra bialkali photocathode (43% quantum efficiency) and improved efficiency in first dynode charge collection like R11265 (83%) should permit to obtain an increase in energy resolution of about 30% respect to a standard bialkali photomultiplier.

Regarding PET applications, the results with LSO(Ce) coupled with multi anode photomultipliers were not only comparable, but even better than the ones obtained with semiconductor devices.

Furthermore the independence from a cooler system and the possibility to assemble easily multiple detectors achieving high performances in terms of spatial resolution, put the new generation of high quantum efficiency multi anode photomultipliers at the top of the current photodetectors.

Acknowledgments

The authors wish to thank Hamamatsu Photonic inc. for providing the R11265 prototype and in particular Ing. F. Giovenale for his kind collaboration. Moreover authors want also to thank without implications Dr Cristina Centioli for her indispensable help in the final draft of the paper.

References

[1] P. Busca, R. Peloso, C. Fiorini, A. Gola, R. Eckhardt, K. Hermenau, P. Lechner, H. Soltau, L. Struder, Nuclear Instruments and Methods in Physics Research Section A: Accelerators, Spectrometers, Detectors and Associated Equipment 624 (2010) 282.
[2] C. Fiorini, A. Gola, M. Zanchi, A. Longoni, H. Soltau, L. Struder, Nuclear Instruments and Methods in Physics Research Section A: Accelerators, Spectrometers, Detectors and Associated Equipment 571 (2007) 126.
[3] C. Fiorini, F. Perotti, Review of Scientific Instruments 76 (2005) 044303.
[4] T. Ikagawa, J. Kataoka, Y. Yatsu, T. Saito, Y. Kuramoto, N. Kawai, M. Kokubun, T. Kamae, Y. Ishikawa, N. Kawabata, Nuclear Instruments and Methods in Physics Research Section A: Accelerators, Spectrometers, Detectors and Associated Equipment 538 (2005) 640.
[5] R. Scafè, R. Pani, R. Pellegrini, G. Iurlaro, L. Montani, M.N- Cinti, Nuclear Instruments and Methods in Physics Research Section A: Accelerators, Spectrometers, Detectors and Associated Equipment 571 (2007) 355.
[6] A. Persson, B. Cederwall, Nuclear Instruments and Methods in Physics Research Section A: Accelerators, Spectrometers, Detectors and Associated Equipment 648 (Sup.1) (2011) S272–S274.
[7] N. Otte, B. Dolgoshein, J. Hose, S. Klemin, E. Lorenza, R. Mirzpyan, E. Popova, M. Teshima, Nuclear Physics B 150 (2006) 417.
[8] A. Kolb, E. Lorenz, M.S. Judenhofer, D. Renker, K. Lankes, Physics in Medicine and Biology 55 (2010) 1832.
[9] E.E. Ovechkina, V. Gaysinskiy, S.R. Millera, C. Brecher, A. Lempicki, V.V. Nagarkara, Radiation Measurements 42 (2007) 541.
[10] A. Gola, C. Fiorini, M. Porro, M. Zanchi, Nuclear Instruments and Methods in Physics Research Section A: Accelerators, Spectrometers, Detectors and Associated Equipment 571 (2007) 339.
[11] Hamamatsu Photonics KK, Electron Tube Center, Japan, (2012) Plot no. TPMH1305E05.
[12] R. Pani, A. Bigongiari, F. Catarsi, M.N. Cinti, G. Iurlaro, M. Meoni, L. Montani, G. Passuello, R. Pellegrini, M. Pieracci, A. Stefanini, Nuclear Instruments and Methods in Physics Research Section A: Accelerators, Spectrometers, Detectors and Associated Equipment 518 (2004) 380.
[13] R. Pani, R. Pellegrini, M. Betti, G. De Vincentis, M.N. Cinti, P. Bennati, F. Vittorini, V. Casali, M. Mattioli, V. Orsolini Cencelli, F. Navarria, D. Bollini, G. Moschini, G. Iurlaro, L. Montani, F. de Notaristefani, Nuclear Instruments and Methods in Physics Research Section A: Accelerators, Spectrometers, Detectors and Associated Equipment 571 (2007) 475.
[14] R. Pani, R. Pellegrini, F. Scopinaro, A. Soluri, G. De Vincentis, A. Pergola, F. Iacopi, A. Corona, A. Grammatico, S. Filippi, P.L. Ballesio, Nuclear Instruments and Methods in Physics Research Section A: Accelerators, Spectrometers, Detectors and Associated Equipment 392 (1997) 295.
[15] R. Pani, R. Pellegrini, M.N. Cinti, P. Bennati, M. Betti, F. Vittorini, M. Mattioli, G. Trotta, V. Orsolini Cencelli, R. Scafè, L. Montani, F. Navarria, D. Bollini, G. Baldazzi, G. Moschini, P. Rossi, F. de Notaristefani, Nuclear Instruments and Methods in Physics Research Section A: Accelerators, Spectrometers, Detectors and Associated Equipment 572 (2007) 268.
[16] R. Pani, R. Pellegrini, M.N. Cinti, P. Bennati, A. Fabbri, S. Ridolfi, R. Scafe, G. De Vincentis, E. Di Castro, N.S.A. Polli, M Caratozzolo, M. Mattioli, P. Boccaccio, G. Moschini, N. Lanconelli, S. Lo Meo, F. Navarria, D. Sacco, V.O. Cencelli, T. Baroncelli, F. de Notaristefani, Nuclear Physics B—Proceedings Supplements 215 (2011) 319.
[17] P. Dorenbos, J.T.M. de Haas, C.W.E. van Eijk, IEEE Transactions on Nuclear Science ED NS51 (2004) 1289.
[18] A. Fabbri, V. Orsolini Cencelli, P. Bennati, M.N. Cinti, R. Pellegrini, G. De Vincentis, R. Pani, Journal of Instrumentation 8 (2013) C02022.
[19] M.N. Cinti, R. Pani, P. Bennati, R. Pellegrini, R. Scafè, A. Fabbri, C. Orlandi, S. Ridolfi, IEEE Nuclear Science Symposium Conference Record, (2011). pp. 1665–1668.
[20] M. Moszynski, Ł. Swiderski, T. Szczesniak, A. Nassalski, A. Syntfeld-Kazuch, W. Czarnacki, G. Pausch, J. Stein, P. Lavoute, F. Lherbert, F. Kniest, Nuclear Science Symposium Conference Record, (2007). pp. 1351–1357.
[21] R Scafé, R. Pani, R. Pellegrini, P. Bennati, M.N. Cinti, G De Vincentis, E. Di Castro, Nuclear Instruments and Methods in Physics Research Section A: Accelerators, Spectrometers, Detectors and Associated Equipment 643 (2011) 89.
[22] M. Moszyński, J. Zalipska, M. Balcerzyk, M. Kapusta, W. Mengesha, J.D. Valentine, Nuclear Instruments and Methods in Physics Research Section A: Accelerators, Spectrometers, Detectors and Associated Equipment 484 (1–3) (2002) 259.
[23] M. Balcerzyk, M. Moszyÿski, M. Kapusta, D. Wolski, J. Pawelke, C.L. Melcher, IEEE Transactions on Nuclear Science ED NS47 (4) (2000) 1319.
[24] A. Del Guerra, N. Belcari, M.G. Bisogni, a F. Corsi, M. Foresta, P. Guerra, S. Marcatili, A. Santos, Gi. Sportelli, Nuclear Instruments and Methods in Physics Research Section A: Accelerators, Spectrometers, Detectors and Associated Equipment 648 (2011) S232.